Table 2. Selected bond distances and angles from the refinement at 293 K. Numbers in parentheses represent standard deviations.

Bond	Distance (Å)	Bond angle	Size (deg)
Zr1–O1	2.042(4)	O1–Zr1–O1	91.44(21)
Zr1–O2	2.108(4)	O1–Zr1–O2	89.57(13)
		O1–Zr1–O2	87.58(12)
		O2–Zr1–O2	91.44(22)
W1–O1	1.798(3)	O1–W1–O1	116.1(1)
W1–O4	1.709(7)	O1–W1–O4	101.6(2)
W2–O2	1.782(3)	O2–W2–O2	109.7(2)
W2–O3	1.733(8)	O2–W2–O3	109.3(2)
W1–O3	2.386(9)	Zr–O1–W1	154.29(22)
		Zr–O2–W2	171.81(26)

bond angles due to transverse vibrations. This flexibility is shown by lattice energy calculations on model compounds in which the thermal contraction is modeled as being caused by a coupled three-dimensional rotation of the rigid polyhedra that make up the lattice network (*13*). Over a volume range corresponding to that observed up to the phase transition, essentially no change in the overall lattice energy is observed; any increases in the nonbonded anion-anion and cation-cation repulsions due to the contraction are offset by an increase in the W1–O3 attraction.

This result suggests the possibility of low-energy phonon modes in the lattice corresponding to these coupled rotations. Such modes will, by definition, exhibit negative Gruneisen parameters, γ_j (*14*), and their population will lead to a negative contribution to the overall coefficient of thermal expansion (*15–17*). Similar arguments have been applied to rationalize the thermal contraction over narrow temperature ranges in other materials (*12*). The large temperature range of negative thermal expansion in this material suggests that the framework structure of this material is such that the overall effective Gruneisen parameter, γ_{eff} (*14*) (which will include contributions from all active modes, both the low-energy transverse modes that tend to contract the lattice and the higher energy longitudinal modes that tend to expand the lattice), remains negative at all temperatures.

The anisotropic thermal vibrations present in ZrW_2O_8 and HfW_2O_8, which cause negative thermal expansion, are presumably present in many other materials, but they are overwhelmed by the more familiar forces that cause positive thermal expansion. Negative thermal expansion cannot be expected in a material unless the distances between bonded atoms increase very little with increasing temperature. Such small changes with temperature occur only in oxides of cations with relatively high formal charge and low coordination number (*18*), which lead to a highly covalent bond. The vibration of O will only produce a significant contribution to negative thermal expansion when it has a coordination number of 2. The metal-oxygen network must also be close to charge-neutral. Charged networks contain interstitial ions, and the ionic bonds between these interstitial ions and the network will have significant positive thermal expansion (*18*). A prerequisite for negative thermal expansion is thus a highly covalent, charge-neutral network with O in twofold coordination.

REFERENCES AND NOTES

1. R. Roy, D. K. Agrawal, H. A. McKinstry, *Annu. Rev. Mater. Sci.* **19**, 59 (1989).
2. A. W. Sleight, *Endeavour* **19**, 64 (1995).
3. V. Korthuis *et al.*, *Chem. Mater.* **7**, 412 (1995).
4. T. A. Mary, V. Korthuis, N. Khosrovani, A. W. Sleight, in *Low Expansion Materials*, D. P. Stinton and S. Y. Limaye, Eds. (American Ceramic Society, Westerville, OH, 1995), vol. 32, pp. 81–85.
5. J. Graham, A. D. Wadsley, J. H. Weymouth, L. S. Williams, *J. Am. Ceram. Soc.* **42**, 570 (1959).
6. L. L. Y. Chang, M. G. Scroger, B. Phillips, *ibid.* **50**, 211 (1967).
7. C. Martinek and F. A. Hummel, *ibid.* **51**, 227 (1968).
8. V. K. Trunov and L. M. Kovba, *Russ. J. Inorg. Chem.* **12**, 1703 (1967).
9. J. S. O. Evans, T. A. Mary, A. W. Sleight, in preparation.
10. According to the method of I. D. Brown and K. K. Wu [*Acta Crystallogr. Sect. B* **32**, 1957 (1976)], valence calculations show this interaction to contribute approximately 5% of the total bonding around W1 and 15% of the bonding around O3.
11. Synthesis of ZrW_2O_8 requires several days of heating at about 1500 K (*5–7*). Even then, the reaction between ZrO_2 and WO_3 is not complete. Synthesis of ZrW_2O_8 is further complicated by the fact that volatilization of WO_3 is pronounced at such high temperatures. We have discovered precursor approaches that allow synthesis of single-phase ZrW_2O_8 with heating times shorter than 2 hours. One such approach yields ZrW_2O_8 at temperatures as low as 850 K, where ZrW_2O_8 is actually metastable. Small crystals suitable for x-ray diffraction studies were isolated from a sample that had been heated at 1475 K for 4 hours.
12. A. Bienenstock and G. Burley, *J. Phys. Chem. Solids* **24**, 1271 (1963).
13. J. D. Gale, GULP (General Utility Lattice Program), Royal Institution of Great Britain, London, 1993.
14. The Gruneisen parameter γ_j is defined as $\gamma_j = d\ln\nu_j/d\ln V$, where ν is the frequency of the *j*th normal mode and *V* is the volume. Population of modes with a negative γ_j will give rise to a decrease in the overall volume. The overall Gruneisen parameter

$$\gamma_{\text{eff}} = \sum_j \gamma_j \exp(-h\nu_j/kT) / \sum_j \exp(-h\nu_j/kT)$$

represents a weighted average over all the populated normal modes, both those with negative (contracting) and those with positive (expanding) contributions to the overall volume.

15. T. H. K. Barron, *Ann. Phys.* **1**, 77 (1957).
16. M. Blackman, *Philos. Mag.* **9**, 831 (1958).
17. G. K. White, *Contemp. Phys.* **34**, 193 (1993).
18. R. M. Hazen and C. T. Prewitt, *Am. Mineral.* **62**, 309 (1977).

19. Supported by the Oregon Metals Initiative, Teledyne Wah Chang Albany, NSF, and the U.S. Department of Energy.

29 November 1995; accepted 19 January 1996

Homogeneous NMR Spectra in Inhomogeneous Fields

Sujatha Vathyam, Sanghyuk Lee, Warren S. Warren*

Researchers interested in high-resolution nuclear magnetic resonance (NMR) spectroscopy have long sought higher magnetic fields to enhance resolution and simplify spectra. Magnets with substantially larger fields than those available in the best commercial spectrometers are available, but the inhomogeneity is unacceptable for high-resolution spectra. A detection method (termed HOMOGENIZED) is presented that removes inhomogeneity while retaining chemical shift differences and *J* couplings. With existing inhomogeneous magnets, this method could nearly double the largest resonance frequency available for high-resolution NMR. The HOMOGENIZED sequence is based on observations of intermolecular zero-quantum coherences between a solute molecule and solvent molecules that are micrometers away; as long as the field is homogeneous over this short distance, sharp resonances are recovered without echoes. Experimental demonstrations and a detailed density matrix theory to explain the effect are presented.

For decades, spectroscopists studying high-resolution NMR have sought ever higher magnetic fields, largely because the spectral width (dominated by chemical shifts) is linearly proportional to the field strength and the intrinsic (homogeneous) linewidth depends only weakly on field strength. Hence, higher fields imply better resolution, as long as inhomogeneous broadening from magnetic field nonuniformity can be neglected. Extremely good homogeneity (on the order of 1 part in 10^9) is needed and has traditionally been achieved by sample spinning and by adjusting a large number of shim coils (additional coils used to homogenize the field). As a result, commercial high-resolution spectrometers today operate at fields up to ~18 T (750-MHz proton resonance frequency), higher by about a factor of 25 than in the pioneering NMR experiments half a century ago.

Magnets with substantially higher fields

Department of Chemistry, Princeton University, Princeton, NJ 08544, USA.

*To whom correspondence should be addressed.

can be built, but such magnets have not been used for high-resolution applications. Materials limitations force compromises in superconducting magnet design at fields much greater than the current values, and these compromises strongly affect the ultimate achievable homogeneity. It is considered unlikely that superconducting magnets with fields greater than 23 T are even possible until new materials become available (*1*). Resistive magnets that use a modified Bitter design can operate with higher fields (*2*), but the homogeneity is much poorer than high-resolution standards. A typical illustration is provided by the 27-T magnet at the National High Magnetic Field Laboratory (NHMFL) (*1*), which has a homogeneity of 100 parts per million per millimeter (ppm/mm) and drifts about 5 ppm/min. In more recent work at NHMFL (*3*) with a 24.6-T magnet, the inhomogeneity has been reduced to ~1 ppm/mm; magnets under construction are expected to reduce the inhomogeneity to 1 ppm over a 1-cm^3 volume and to reduce the drift to a comparable amount during data acquisition (*1*). Unfortunately, this development still implies an inhomogeneous linewidth tens or hundreds of times greater than the homogeneous width in solution, eliminating any resolution advantage.

Inhomogeneous broadening can be removed by a variety of techniques, but none is completely satisfactory for high-resolution NMR. The spin echo sequence $(90-\tau-180-\tau)$ (*4*) or multiple-pulse sequences such as the Carr-Purcell sequence $[90_x-(\tau-180_x-2\tau-180_x-\tau)_n]$ (*5*) remove inhomogeneous broadening, but they also completely remove chemical shifts and *J* couplings if τ is much shorter than the reciprocal of the coupling constants. When τ gets longer, these sequences produce a grossly distorted spectrum. More recently, it has been shown that intramolecular zero-quantum (ZQ) coherences (which connect states with the same number of spins up, for example, $\alpha\alpha\beta$ and $\beta\alpha\alpha$) are insensitive to magnetic field inhomogeneity (*6*). Unfortunately, ZQ coherences cannot be observed in a normal single-pulse free induction decay, and the ZQ spectrum is much more difficult to interpret than the normal spectrum. For example, isolated spins (singlets) do not give ZQ coherences, and calculating the intensity of ZQ coherences from coupled spins requires a full density matrix simulation of the pulse sequence.

However, intermolecular ZQ coherences—flipping up one solute spin while simultaneously flipping down a nearby solvent spin—would give a very simple spectrum. As long as the magnetic field is homogeneous over the distance between the two spins, this ZQ spectrum would be just the conventional single-quantum spectrum of the solute, shifted by the chemical shift of the solvent. Thus, chemical shift differences and coupling information for the solute could be retained, yet inhomogeneous broadening would be eliminated; field drift would be almost completely canceled as well. Unfortunately, in conventional NMR theory, preparation of ZQ coherences explicitly requires a coupling between the two spins. Because the spins are on two different molecules, only the dipole-dipole interaction would provide such a coupling, and this interaction is normally assumed to be averaged away by diffusion. Even if such a state could be prepared, detection of the coherence also requires a coupling. Thus, observing such an intermolecular ZQ spectrum would certainly appear to require heroic means.

We present a method (Fig. 1) that detects such intermolecular ZQ coherences in solution, thus giving high-resolution spectra in extremely inhomogeneous magnetic fields without removing chemical shifts and *J* couplings. We call this detection method the HOMOGENIZED (HOMOGeneity ENhancement by Intermolecular ZEro-quantum Detection) sequence. The effects of the HOMOGENIZED sequence (the portion in the box in Fig. 1A) after single-pulse excitation are demonstrated in Figs. 2 to 4. A sample of 5% methyl ethyl ketone (MEK) in acetone was chosen. The conventional ^{1}H spectrum of this sample is shown in Fig. 2A; the sample was then deshimmed to produce a linewidth of ~85 Hz (Fig. 2B). The sequence in Fig. 1A was applied to the deshimmed sample, resulting in the ZQ spectrum shown in Fig. 3A at a relatively high contour level. The ZQ peaks in the F_1 dimension are narrow and well resolved, at frequencies $\nu_{\mathrm{acetone}} - \nu_{\mathrm{MEK}}$ (corresponding to solute-solvent ZQ coherences) and at $F_1 = 0$ Hz (corresponding to solvent-solvent ZQ coherences). The multiplicity of the peaks is retained in F_1, as seen in an expanded view of the ZQ cross peak ($\nu_{\mathrm{acetone}} - \nu_{\mathrm{MEK\ triplet}}$), which is a triplet (Fig. 4), and in the ZQ cross peak ($\nu_{\mathrm{acetone}} - \nu_{\mathrm{MEK\ quartet}}$), which is a quartet. The linewidth of each of the peaks in the ZQ triplet at ($F_1 = 660$ Hz, $F_2 = -560$ Hz) is around 4.5 Hz along F_1, with a resolution of 1 Hz (Fig. 4). The one-dimensional (1D) ^{1}H spectrum can be obtained from this two-dimensional (2D) ZQ spectrum by adding the chemical shift of the solvent peak to all of the cross peaks.

The HOMOGENIZED detection method is related to recent experiments that use gradient echoes to detect intermolecular multiple-quantum coherences in samples with at least one concentrated component (such as proteins in water) (*7–12*). For example, the CRAZED sequence, which is a correlated spectroscopy (COSY) sequence modified to include an *N*-quantum coherence transfer echo around the second radio-frequency (rf) pulse (Fig. 1C), gives strong peaks in the indirectly detected dimension that have

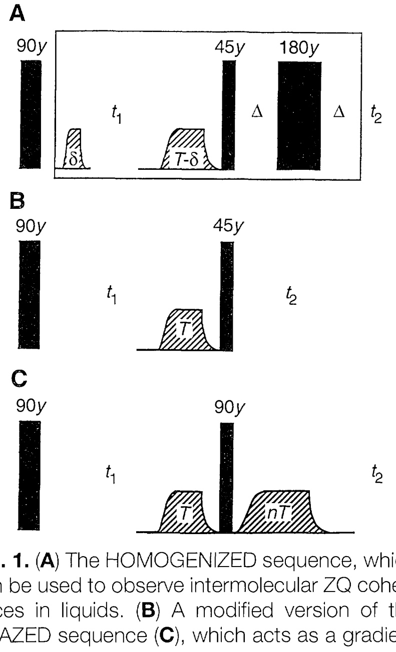

Fig. 1. (**A**) The HOMOGENIZED sequence, which can be used to observe intermolecular ZQ coherences in liquids. (**B**) A modified version of the CRAZED sequence (**C**), which acts as a gradient filter, enabling observation of ZQ coherences only. The HOMOGENIZED sequence improves on the sequence in (B) by compensating for radiation damping and large inhomogeneities (see text).

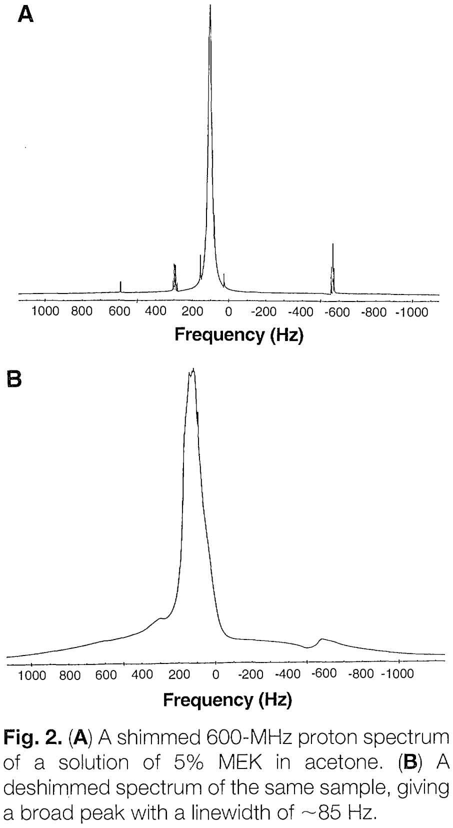

Fig. 2. (**A**) A shimmed 600-MHz proton spectrum of a solution of 5% MEK in acetone. (**B**) A deshimmed spectrum of the same sample, giving a broad peak with a linewidth of ~85 Hz.

all of the experimental properties of N-quantum coherences between independent molecules (*7*). In principle, simply leaving out the second gradient pulse selects for ZQ coherences. However, the CRAZED sequence gives only a very weak ZQ signal. For simplicity here we first ignore intramolecular couplings, relaxation processes, and radiation damping and restrict ourselves to z-gradients. The full Hamiltonian for N spins in the presence of a gradient G in the s direction is then

$$\mathcal{H} = \hbar\sum_{i=1}^{N}[\Delta\omega_i + (\gamma G s_i)]I_{zi} + \hbar\sum_{i=1}^{N}\sum_{\substack{j=1\\ j\neq i}}^{N} D_{ij}(3I_{zi}I_{zj} - \mathbf{I}_i\cdot\mathbf{I}_j) \qquad (1)$$

$$D_{ij} = \frac{\mu_0}{4\pi}\frac{\gamma^2\hbar}{4}\frac{1-3\cos^2\theta_{ij}}{r_{ij}^3} \quad \text{if } r_{ij} > r_0;\ D_{ij} = 0 \text{ otherwise} \qquad (2)$$

The first sum on the right in Eq. 1 reflects the interaction with the external field and gradient; $\hbar$ is Planck's constant divided by 2π, and $\Delta\omega_i$ is the resonance offset of the ith spin (which will also depend on position if there is inhomogeneous broadening). The second term is the secular part of the dipole-dipole interaction; D_{ij} is the dipolar coupling constant, r_{ij} is the separation between spin i and j, θ_{ij} is the angle between the internuclear vector and the applied magnetic field $B_0\hat{\mathbf{z}}$, γ is the gyromagnetic ratio, and μ_0 is the vacuum permeability. The dipole-dipole interaction is usually assumed to be averaged out by molecular diffusion in solution NMR. However, as noted (*7*), only the short-range dipolar couplings are motionally averaged out; the dipolar coupling between spins separated by much more than the distance molecules diffuse on an NMR time scale ($r_0 \approx 10$ μm) should be retained. The surviving dipolar couplings are quite small ($<10^{-8}$ rad s^{-1}), but the very large number of spins generates an easily observable effect. The assumption of an arbitrary distance r_0 is useful for emphasizing the role of long-range couplings, but in fact it has no effect on the final result; we show elsewhere that all of the dipolar couplings satisfy the condition $|D_{ij}T| \ll 1$, where T is the length of time spins i and j can coherently interact (limited either by relaxation or diffusion), and this restriction is sufficient to calculate the evolution analytically (*11*).

The observable signal can be calculated analytically, if effects such as radiation damping and relaxation are ignored. We start (*11*) with the equilibrium density matrix ρ_{eq} for N spin-1/2 nuclei without the high-temperature approximation

$$\rho_{eq} = 2^{-N}\prod_i(1 - \mathfrak{F}I_{zi});\ \mathfrak{F} = 2\tanh(\hbar\omega_0/2kT) \qquad (3)$$

where kT is the thermal energy and I_{zi} is the operator for z-magnetization on spin i. Starting from ρ_{eq}, the density matrix after a $(\pi/2)$ pulse is

$$\rho_{eq} = 2^{-N}\prod(1 - \mathfrak{F}I_{xi}) \qquad (4)$$

which contains intermolecular ZQ operators in the $\mathfrak{F}^2$ term and higher terms, because

$$I_{xi}I_{xj} = \tfrac{1}{2}[(I_{xi}I_{xj} + I_{yi}I_{yj}) + (I_{xi}I_{xj} - I_{yi}I_{yj})]$$

$$= \tfrac{1}{4}[(I_{+i}I_{-j} + I_{-i}I_{+j}) + (I_{+i}I_{+j} - I_{-i}I_{-j})] \qquad (5)$$

During t_1 the term $I_{+i}I_{-j}$ evolves at the difference of resonance offsets, $\Delta\omega_i - \Delta\omega_j$; during the gradient pulse, this term evolves at $(\Delta\omega_i + \gamma G s_i) - (\Delta\omega_j + \gamma G s_j)$. At the end of the first gradient pulse, the ZQ component of the $\mathfrak{F}^2$ term will then be

$$2^{-N-1}\mathfrak{F}^2\sum_{i>j}\{(I_{+i}I_{-j} + I_{-i}I_{+j}) \times \cos[(\Delta\omega_i - \Delta\omega_j)(t_1+T) + \gamma G(s_i - s_j)T]\} \qquad (6)$$

In a CRAZED sequence, the second $\pi/2$ pulse translates some fraction of the desired multiple-quantum coherences into single-quantum coherences, which are then made observable by dipolar couplings. However, none of this ZQ coherence is made observable by a $\pi/2$ pulse, because

$$I_{+i}I_{-j} + I_{-i}I_{+j} = 2(I_{xi}I_{xj} + I_{yi}I_{yj}) \xrightarrow{\pi/2\ \text{pulse}} 2(I_{yi}I_{yj} + I_{zi}I_{zj}) \qquad (7)$$

which is entirely zero- and double-quantum coherences.

In fact, the time evolution to all powers of $\mathfrak{F}$ can be evaluated (*11*). Ignoring radiation damping and relaxation, the signal for an n-quantum CRAZED sequence is

$$M^+(t_1,t_2) = i^{n-1}e^{i\Delta\omega t_2}e^{-in\Delta\omega t_1}M_0 n\left(\frac{\tau_d}{t_2\Delta_s}\right)J_n\left(-\frac{t_2\Delta_s}{\tau_d}\right) \qquad (8)$$

where M_0 is the equilibrium magnetization, $\tau_d = (\gamma\mu_0 M_0)^{-1}$ is the dipolar demagnetizing time (≈70 ms for pure water at room temperature in a 600-MHz spectrometer), $\Delta_s = [3(\hat{s}\cdot\hat{z})^2 - 1]/2$, and J_n is the nth-order Bessel function. The function in Eq. 8 vanishes if $n = 0$. Hence, the ZQ version of CRAZED is not directly useful.

However, replacing the second $\pi/2$ pulse with a $\pi/4$ pulse (Fig. 1B) does transfer some ZQ coherence into single-quantum operators:

$$I_{+i}I_{-j} + I_{-i}I_{+j} = 2(I_{xi}I_{xj} + I_{yi}I_{yj}) \xrightarrow{\pi/4\ \text{pulse}} 2I_{yi}I_{yj} + \tfrac{1}{2}(I_{zi}I_{zj} + I_{xi}I_{xj} + I_{zi}I_{xj} + I_{xi}I_{zj}) \qquad (9)$$

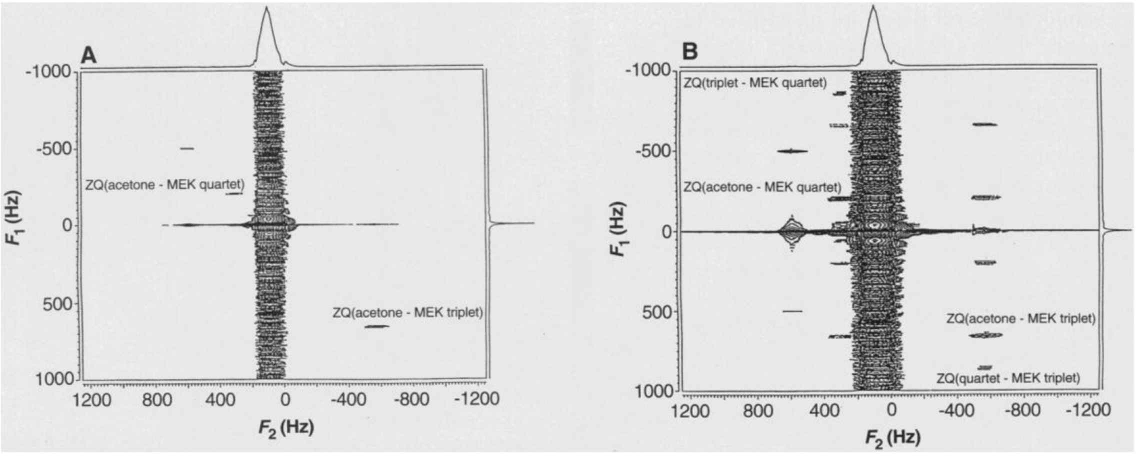

Fig. 3. (**A** and **B**) The 2D ZQ spectrum obtained with the HOMOGENIZED sequence shown in Fig. 1A. The gradient pulse at the beginning of t_1 was 0.5 ms with a strength of 12 G cm^{-1}; the gradient pulse at the end of t_1 was 1 ms with a strength of 30 G cm^{-1}; Δ was 40 ms. A marked reduction in the linewidths is seen in the indirectly detected dimension. Intermolecular ZQ peaks are observed between acetone (the solvent) and the triplet and quartet of MEK, respectively, at frequencies corresponding to ($F_1 = \nu_{acetone} - \nu_{MEK}$, $F_2 = \nu_{MEK}$). (B) The same spectrum at a lower contour level shows cross peaks between acetone and the quartet, at the F_2 frequency of the quartet as well as at that of the triplet, due to J coupling between the triplet and the quartet. The 1D proton spectrum of MEK can be obtained from this 2D spectrum, by removal of the chemical shift due to the acetone.

We normally use gradient pulses that are strong enough to dephase bulk magnetization ($\gamma GTR \gg 1$, where R is the length of the sample in the gradient direction) and overwhelm inhomogeneous broadening [$(\Delta\omega_i - \Delta\omega_j)t_2 \ll 1$ and $(\Delta\omega_i - \Delta\omega_j)(t_1 + T) \ll 1$ for solvent spins separated by a distance d such that $\gamma GTd \approx \pi$] but not so strong that the magnetization helix is eliminated by diffusion ($\gamma GTr_0 \ll 1$). In Box 1 we use the methods detailed in (*11*) to derive an essentially exact expression, in this case for the observable part of the density matrix, including all powers of $\mathfrak{F}$:

$$\rho^{\text{obs}} = -2^{-(N+1/2)}\mathfrak{F}\sum_{i=1}^{N}[I_{yi}\cos(\Delta\omega_i t_2) - I_{xi}\sin(\Delta\omega_i t_2)]\mathbf{J}_1\left(\frac{-t_2\Delta_s}{\sqrt{2}\tau_d}\right) \tag{10}$$

The signal

$$M^+(t_1,t_2) = Tr\Big[\rho\gamma\hbar\sum_i(I_{xi} + iI_{yi})\Big] \tag{11}$$

reaches a maximum value when $t_2 = 2.6\ \tau_d$ of 41% of the magnetization immediately after a single 90° pulse. The signal for the solvent-solute cross peaks follows a similar derivation, except that only the terms $D_{ij}(I_{xi}I_{xj} + I_{yi}I_{yj})$ can be omitted from the Hamiltonian in Eq. 1; the net effect is that the signal only grows in two-thirds as fast.

The HOMOGENIZED sequence (Fig. 1A) derives from the sequence described above, with two important modifications. Equation 10 shows that the density matrix retains the full inhomogeneous broadening during t_2. The magnetization requires a time on the order of τ_d to appear, and, if the inhomogeneity is substantial, the magnetization will dephase before the dipolar Hamiltonian can do its work. Thus, we insert a simple spin echo (which does not remove dipolar interactions) at the beginning of the detection period to refocus the solvent magnetization.

In addition, we have ignored radiation damping in this entire analysis. In a normal probe with concentrated solvent, radiation damping during t_1 will rotate the solvent magnetization back toward equilibrium and will significantly reduce the signal unless the bulk magnetization is eliminated quickly ($\ll$10 ms) after the first 90° pulse. Putting the gradient pulse at the beginning of t_1 would do this, but then diffusion during t_1 would limit the achievable resolution by wiping out the magnetization grating. Thus, a better solution is to give an intense but brief gradient pulse at the beginning of t_1, with the bulk of the gradient at the end of t_1. In addition, the spectra in Figs. 2 to 4

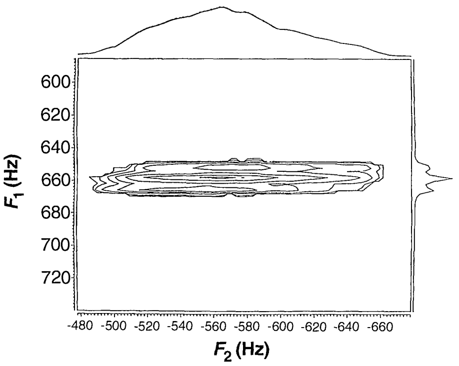

Fig. 4. An expanded view of the ZQ cross peak at ($F_1 = \nu_{\text{acetone}} - \nu_{\text{MEK triplet}}$, $F_2 = \nu_{\text{MEK triplet}}$). It is very well resolved in F_1, showing the triplet structure, despite starting out as an indistinguishable wide peak in F_2. Inhomogeneous broadening is removed without removing chemical shift and *J*-coupling information.

Box 1. The density matrix methods detailed in (*11*) can be used to solve for the complete evolution for the pulse sequence in Fig. 1B. Here we show the simplest case (the solvent-solvent ZQ peak) to demonstrate how the signal grows in. Starting from Eq. 3, we find that the dipolar Hamiltonian can be ignored until the beginning of t_2, giving

$$\rho(t_1,t_2 = 0)\ 2^{-N}\prod_i\Bigg\{1_i + \mathfrak{F}\left(\frac{I_{zi} - I_{xi}}{\sqrt{2}}\right) \times \cos[\Delta\omega_i(t_1 + T) + \gamma GTs_i] - \mathfrak{F}I_{yi}\sin[\Delta\omega_i(t_i + T) + \gamma GTs_i]\Bigg\}$$

Spatial averaging eliminates all terms that depend on absolute position (instead of relative positions such as $s_i - s_j$), including all terms containing odd powers of $\mathfrak{F}$. The only $\mathfrak{F}^2$ term that survives is

$$-\tfrac{1}{4}\,I_{xi}I_{zj}\cos[(\Delta\omega_i - \Delta\omega_j)(It_1 + T)]\cos[\gamma GT(s_i - s_j)]$$

For higher powers of $\mathfrak{F}$ in this "homomolecular" case, the terms $D_{ij}\mathbf{I}_i\cdot\mathbf{I}_j$ in the dipolar Hamiltonian (Eq. 1) contribute no signal, and only product operators with exactly one transverse operator (I_{yi} or I_{xi}) are ever made into observable magnetization by dipolar couplings in t_2. In general, the term proportional to $\mathfrak{F}^{2n}$ that will become observable after ($2n - 1$) commutations with the $D_{ij}I_{zi}I_{zj}$ terms from the Hamiltonian has the form

$$\mathfrak{F}^{2n}\ \overbrace{I_{xi}I_{zj}I_{zk}\ldots}^{2n\text{ terms}}\begin{Bmatrix}\cos[(\Delta\omega_i - \Delta\omega_j)(t_1 + T)]\cos[(\Delta\omega_i - \Delta\omega_k)(t_i + T)]\ldots\\ \times\cos[\gamma GT(s_i - s_j)]\cos[\gamma GT(s_i - s_k)]\ldots\end{Bmatrix}$$

and gives

$$-2^{-N}\frac{\mathfrak{F}^{2n}t_2^{2n-1}}{2^{3n-1}n!(n-1)!}\sum_{i=1}^{N}(-1)^{n-1} \times I_{yi}\left\{\tfrac{3}{2}\sum_{j=1}^{N}D_{ij}\cos[(\Delta\omega_i - \delta\omega_j)(t_1 + T)]\cos[\gamma GT(s_j - s_i)]^{2n-1}\right\}$$

plus multiple-spin terms. Adding up all the observable terms in all powers of $\mathfrak{F}$ gives

$$\rho^{\text{obs}} = -2^{-(N+1/2)}\mathfrak{F}\sum_{i=1}^{N}I_{yi}\sum_{n=1}^{N/2}\frac{(-1)^{n-1}}{n!(n-1)!}\Lambda^{2n-1}$$

where

$$\Lambda \equiv \mathfrak{F}t_2 \times \frac{3}{4\sqrt{2}}\sum_{j=1}^{N}D_{ij} \times \cos[(\Delta\omega_i - \Delta\omega_j)(t_1 + T)]\cos[\gamma GT(s_j - s_i)]$$

This is simplified by substituting for the Bessel function

$$J_v(x) = \sum_{k=0}^{\infty}\frac{(-1)^k}{k!(v + k)!}\left(\frac{x}{2}\right)^{v+2k}$$

and noting (*8, 11*) that

$$\sum_{j=1}^{N}D_{ij}\cos[(\Delta\omega_i - \Delta\omega_j)(t_1 + T)]\cos[\gamma GTs_j] \approx \frac{N}{V}\frac{\mu_0\hbar\gamma^2}{6}\Delta_s$$

Hence

$$\rho^{\text{obs}} = -2^{-(N+1/2)}\,\mathfrak{F}\sum_{i=1}^{N}I_{yi}\mathbf{J}_1\left(\frac{-t_2\Delta_s}{\sqrt{2}\tau_d}\right)$$

On including the chemical shift evolution during t_2, we get Eq. 10.

were taken with $\Delta = 40$ ms ($\approx 0.4\ \tau_d$), shorter than the optimal value predicted above, to further reduce diffusion effects. Our experimental signals are about 10% of the full magnetization, and adjusting pulse sequence parameters could probably improve this further. Incidentally, we see some signal even for a ZQ CRAZED, presumably due to radiation damping; the rf pulse created by the precessing solvent magnetization destroys the argument in Eq. 7 that no single-quantum operators are produced.

The quantum picture also explains why at a very low contour level (Fig. 3B) other peaks appear as well. For example, at $F_2 = \nu_{\text{MEK triplet}}$, apart from the two ZQ cross peaks between acetone and the triplet $[F_1 = \pm(\nu_{\text{acetone}} - \nu_{\text{MEK triplet}})]$, we also see the two cross peaks between acetone and the quartet, $[F_1 = \pm(\nu_{\text{acetone}} - \nu_{\text{MEK quartet}})]$. These are the traditional COSY cross peaks due to *J* coupling between the triplet and the quartet, except that the coherence during t_1 also involves flipping down one solvent spin. The simplest way to get an inhomogeneity-free spectrum is to just sum over the different F_2 slices, in which case these extra peaks actually enhance the observed signal.

For the CRAZED sequence it is possible to view the effects of dipolar couplings by introducing a dipolar demagnetizing field $\mathbf{B}_d(s)$ and then allowing this field to give an additional contribution $\mathbf{M}(s) \times \gamma\mathbf{B}_d(s)$ to the Bloch equations (*7, 10, 13*). When $t_1 = t_2 = 0$ and $n > 1$ for the CRAZED sequence in Fig. 1C, the sequence reduces to a multiple spin echo, first explored (*14, 15*) in ^{3}He by Deville *et al.* (who introduced the demagnetizing field framework) and recently in more conventional samples such as pure water (*16–18*). However, there is no "zeroth spin echo" ($t_1 = t_2 = n = 0$), which would correspond to the effect we discuss here, even for long gradient pulses. Still, a corrected version of the demagnetizing field approach (*10*) turns out to be valid for numerical calculations and will give the same results in solution as the quantum picture described here (*11*). In related work, Jeener *et al.* (*19*) have developed an iterative approach to solving modified Bloch-Redfield equations to connect the quantum and classical pictures, and although only low orders of iteration have been solved to date, it seems quite likely that this approach will converge to the same results as well.

The HOMOGENIZED detection sequence can be useful in more conventional magnets. Samples with strong solvent peaks (such as proteins in water) are difficult to shim because the solvent contributes its own dipolar demagnetizing field. This demagnetizing field consists of a time-independent part (*20*) (arising, for example, from the magnetic susceptibility of the molecules; this part is generally shimmed or spun away) and a potentially time-dependent part (arising from dipolar couplings with all other spins, which might flip during the experiment). For a typical sample geometry (5-mm cylindrical tube with 1-cm active region), a sample of 80% H_2O in a 14-T (600 MHz) NMR spectrometer would generate a time-dependent demagnetizing field that shifts solute resonances by +2 to −1 Hz, depending on position in the sample. These shifts are directly proportional to the solvent magnetization, and if the magnetization moves during the NMR experiment (as a result of relaxation or the pulse sequence itself), the shifts change. This effect would also be eliminated by the HOMOGENIZED sequence, as would susceptibility broadening in microprobes (*21*) or in structured materials such as tissue (*22*).

A homogeneous ^{1}H 2D spectrum of almost any sample can be obtained with the HOMOGENIZED sequence, as long as at least one component of the sample has concentrated proton magnetization. For the sequence in Fig. 1A the preparation period is a single pulse, but it could just as easily be more complex. A concentrated ^{13}C solvent would permit a homogeneous ^{13}C spectrum of the solute and might even permit homogeneous ^{1}H spectra through the observation of transitions that flip four ^{13}C solvent spins up and one ^{1}H solute spin down (because the ratio of γ values is very close to 4:1). Sensitivity could be improved by putting multiple echo pulses in t_2. Finally, the solvent-solvent peak at $F_1 = 0$ can be eliminated, if necessary, by several different methods; perhaps the simplest, which works well in a protein, is to take advantage of differences in diffusion rates with a gradient echo just before acquisition, as in the DRYCLEAN experiment (*23*). We have recently demonstrated ~95% solvent suppression on, bovine pancreatic trypsin inhibitor (BPTI) samples, while retaining nearly all of the solvent-solute cross-peak intensity (*24*).

Our results demonstrate that intermolecular ZQ coherences can retain chemical shift differences yet suppress inhomogeneous broadening and can produce spectra with substantial and predictable intensities for the allowed transitions. The effect can be calculated either with modified nonlinear (demagnetizing field) Bloch equations or with a full density matrix treatment. However, the HOMOGENIZED sequence represents an excellent example that shows the differences in the intuitive value and predictive power of the two approaches. Because the first pulse rotates the magnetization into the *xy* plane, the dipolar demagnetizing field during t_1 reduces to the form $\mathbf{B}_d(s) = \mu_0\Delta_s\mathbf{M}(s)/3$, which has no effect at all on the time evolution $[\mathbf{M}(s) \times \gamma\mathbf{B}_d(s) = 0]$. Thus, in the classical picture, nothing evolves during t_1 at the homogeneous frequency differences, and there would be no intuitive reason to expect the HOMOGENIZED sequence to work. Although it may sound illogical to NMR spectroscopists, the effect of the demagnetizing field during the t_2 interval is to alter the apparent evolution frequencies during t_1; this is a consequence of the nonlinearities introduced into the Bloch equations by these additions. As we determined in our earlier work, the combination of classical and quantum treatments gives insight and calculational convenience and is better than either treatment alone.

REFERENCES AND NOTES

1. P. L. Kuhns, A. Kleinhammes, W. G. Moulton, N. S. Sullivan, *J. Magn. Reson. A* **115**, 270 (1995).
2. M. D. Bird, S. Bole, Y. M. Eyssa, B. J. Gao, H. J. Schneider-Muntau, *IEEE Trans. Magn.* **30**, 2200 (1994).
3. T. A. Cross, personal communication.
4. E. L. Hahn, *Phys. Rev.* **80**, 580 (1950).
5. H. Y. Carr and E. M. Purcell, *ibid.* **94**, 630 (1954).
6. W. P. Aue, E. Bartholdi, R. R. Ernst, *J. Chem. Phys.* **64**, 2229 (1976); M. Munowitz and A. Pines, *Science* **233**, 525 (1986); R. R. Ernst, G. Bodenhausen, A. Wokaun, *Principles of Nuclear Magnetic Resonance in One and Two Dimensions* (Clarendon, Oxford, 1987).
7. Q. He, W. Richter, S. Vathyam, W. S. Warren, *J. Chem. Phys.* **98**, 6779 (1993).
8. W. S. Warren, W. Richter, A. H. Andreotti, B. T. Farmer II, *Science* **262**, 2005 (1993); W. Richter, S. Lee, W. S. Warren, Q. He, *ibid.* **267**, 654 (1995).
9. D. L. Mattiello, G. T. Montelione, L. Mueller, W. S. Warren, B. T. Farmer II, paper presented at the Experimental NMR Conference, Boston, March 1995; D. L. Mattiello, W. S. Warren, L. Mueller, B. T. Farmer II, *J. Am Chem. Soc.*, in preparation.
10. W. S. Warren, S. Lee, W. Richter, S. Vathyam, *Chem. Phys. Lett.* **247**, 207 (1995).
11. S. Lee, W. Richter, S. Vathyam, W. S. Warren, *J. Chem. Phys.*, in press.
12. P. C. M. van Zijl, M. O'Neill Johnson, S. Mori, R. E. Hurd, *J. Magn. Reson. A* **113**, 265 (1995).
13. G. J. Bowden, T. Heseltine, M. J. Prandolini, *Chem. Phys. Lett.* **233**, 639 (1995).
14. G. Deville, M. Bernier, J. M. Delrieux, *Phys. Rev. B* **19**, 5666 (1979).
15. D. Einzel, G. Eska, Y. Hirayoshi, T. Kopp, P. Wölfle, *Phys. Rev. Lett.* **53**, 2312 (1984).
16. R. Bowtell, R. M. Bowley, P. Glover, *J. Magn. Reson.* **88**, 643 (1990).
17. H. Körber, E. Dormann, G. Eska, *ibid.* **93**, 589 (1991).
18. A. S. Bedford, R. Bowtell, R. M. Bowley, *ibid.*, p. 516.
19. J. Jeener, A. Vlassenbroek, P. Broekaert, *J. Chem. Phys.* **103**, 1309 (1995).
20. T. M. Barbara, *J. Magn. Reson. A* **109**, 265 (1994).
21. D. L. Olson, T. L. Peck, A. G. Webb, R. L. Magin, J. V. Sweedler, *Science* **270**, 1967 (1995).
22. See, for example, C. H. Durney *et al.*, *J. Magn. Reson.* **85**, 554 (1989); C. S. Springer, in *NMR in Physiology and Medicine*, R. J. Gillies, Ed. (Academic Press, Orlando, FL, 1994), pp. 75–99.
23. P. C. M. van Zijl and C. T. W. Moonen, *J. Magn. Reson.* **87**, 18 (1990).
24. S. Vathyam, C. B. Rios, G. Montelione, W. S. Warren, in preparation.
25. Supported under NIH grant GM35253. We thank B. T. Farmer II for helpful discussions and for access to NMR instrumentation at Bristol-Myers Squibb.

3 November 1995; accepted 8 February 1996